Journal of Electronics, Electromedical Engineering, and Medical Informatics
Homepage: jeeemi.org; Vol. 9, No. 1, January 2027, pp: 97-109 e-ISSN: 2656-8632

RESEARCH ARTICLE OPEN ACCESS

LEDI-DRCNET: Leukemia Disease Classification Using a Deep Learning-Based Deep Dilated Residual Convolutional Neural Network

Della Reasa Valiaveetil, and Kanimozhi T

Department of Electronics and Communication Engineering, Vel Tech Rangarajan Dr. Sagunthala R&D Institute of Science and Technology, Avadi, Chennai, India.

Corresponding author: Della Reasa Valiaveetil. (dellareasa@gmail.com), **Author(s) Email:** Kanimozhi T (drtkanimozhi@veltech.edu.in).

Abstract

Background: Leukemia is a hematological malignancy characterized by the abnormal proliferation of progenitor cells in the bone marrow, resulting in irregular white blood cell (WBC) production. Accurate and reliable leukemia classification remains challenging because of variations in cellular morphology, similarities among leukemia subtypes, and the limited availability of training data. These challenges highlight the need for effective automated classification approaches based on microscopic blood cell images.

Aims: This study aims to develop a novel deep learning-based framework, termed LEDI-DRCNET, to improve the accuracy and reliability of leukemia classification using microscopic blood cell images.

Methods: The proposed LEDI-DRCNET framework integrates image preprocessing, segmentation, deep feature extraction, and classification into a unified approach. Initially, Average and Laplacian (AVLA) filters are applied to reduce image noise, enhance image quality, and improve cellular boundary visibility. Subsequently, the Adaptive Region Growing Algorithm (AGRA) is employed to segment WBC regions from microscopic blood cell images. RegNet is then utilized to extract discriminative spatial and structural features from the segmented images. Finally, a Deep Dilated Residual Convolutional Neural Network (DDRCNN) performs multiclass classification into four categories: normal, acute lymphoblastic leukemia (ALL), acute myeloid leukemia (AML), and chronic lymphocytic leukemia (CLL). Classification performance is evaluated and compared with existing machine learning and deep learning approaches.

Results: The proposed LEDI-DRCNET framework achieves an overall classification accuracy of 99.06%, outperforming EfficientNetV2B3, KNN, DenseNet121, and SVM by 1.13%, 1.67%, 0.05%, and 3.17%, respectively. These results demonstrate the effectiveness of the integrated preprocessing, segmentation, feature extraction, and classification framework.

Conclusion: The proposed LEDI-DRCNET framework demonstrates superior classification accuracy compared with the evaluated methods, providing an effective approach for automated leukemia detection and multiclass classification using microscopic blood cell images.

Keywords: Leukemia; Average and Laplacian filter; Adaptive Region Growing Algorithm; RegNet; Deep Dilated Residual Convolutional Neural Network.

I. Introduction

Leukemia (L), a type of blood cancer (BC), affects the replication of white blood cells (WBCs) in the bone marrow. It causes a rise in abnormal WBC, which reduces immunity [1]. The human body is normally made up of three types of cells: red BC, WBC, and platelets [2]. LD is separated into two primary categories: acute leukemia and chronic leukemia. The four main forms of leukemia are chronic myelogenous leukemia (CML), acute lymphocytic leukemia (ALL), acute myelogenous leukemia (AML), and chronic lymphocytic leukemia (CLL) [3]. ALL is the most frequent leukemia in young people, while AML is the most common malignant BC in adults. The World Health Organization (WHO) estimates that around 19 million individuals were diagnosed with cancer in 2020, and 10 million of them died [4]. Cancer is the main cause of death due to its aggressiveness, as well as the complexity and cost of its treatments [5]. Individual differences in leukemia symptoms include frequent or severe infections, nosebleeds, easy bleeding or bruising, and little red spots on the skin [6].

Automated leukemia detection systems, which employ cutting-edge technologies such as image processing (IP), genetic analysis, deep learning, and machine learning, are transforming diagnosis and

Manuscript received 22 September 2025; Accepted 30 March 2026; Available online 22 November 2026
Digital Object Identifier (**DOI**): https://doi.org/10.35882/jeeemi.v9i1.1224
Copyright © 2026 by the authors. This work is an open-access article and licensed under a Creative Commons Attribution-ShareAlike 4.0 International License (CC BY-SA 4.0).

treatment [7] [8]. Among the various DL [9] [10] approaches, Convolutional Neural Networks (CNNs) [11] stand out for their exceptional accuracy and dependability in image classification applications [12]. CNNs [13] are an important component in the creation of automated diagnostic tools because they successfully combine image analysis capabilities with the broader pattern recognition capabilities of Artificial Neural Networks (ANNs) [14] [15]. Automated leukemia detection using machine learning and deep learning techniques have achieved promising results; however, several limitations remain. Many approaches rely on limited and imbalanced datasets, which leads to biased learning and reduces the ability of models to accurately detect minority leukemia subtypes. To overcome this a novel LEDI-DRCNET has been proposed for LD classification. The primary contributions of this research are as follows:

1. The novelty of the proposed method lies in the development of the LEDI-DRCNET framework, which integrates adaptive preprocessing, effective segmentation, deep feature extraction and dilated residual learning for accurate LD classification from microscopic blood cell images.
2. An AVLA hybrid filtering strategy is employed in the preprocessing stage to reduce background noise while enhancing edge contrast, enabling clearer representation of white blood cell boundaries.
3. The AGRA is utilized to accurately segment white blood cells from blood cell images, effectively handling overlapping, irregular and low-contrast cells to improve region extraction.
4. RegNet-based deep feature extraction is incorporated to capture multi-level spatial and structural characteristics of leukemic cells, enabling robust learning of discriminative features.
5. Finally, a DDRCNN with attention mechanisms is designed for leukemia classification, allowing the network to capture multi-scale contextual information and achieve improved diagnostic performance.

The remainder of this paper is organized as follows: The literature survey is summarized in section 2. In section 3, explained the Leukemia classification, in section 4, the result and discussion of the LEDI-DRCNET approach are explained. The conclusion and future work for further investigate are given in section 5.

II. Literature Survey

Researchers have proposed several advanced ML and DL architectures for leukemia classification. SVM, KNN, and GoogLeNet have been used with various techniques and designs for Leukemia classification in the research studies that have been proposed. Some of the researches are examined in the following section. Darmawan et al., [16] proposed an automated framework for identifying and naming cells in microscopic images using the EfficientNetV2B3 model integrated with the Explainable Artificial Intelligence (XAI) technique, LIME. Their approach not only provided accurate predictions but also improved interpretability, achieving an accuracy, F1-score, and average recall of 97.95%. Similarly, Almahdawi et al. [17] introduced a DLNN-based leukemia detection system combined with Particle Swarm Optimization (PSO) for feature optimization. In this method, deep learning was employed for feature extraction, while PSO selected the most relevant features for ML classification. Experimental results demonstrated that the GoogLeNet model integrated with SVM and K-NN classifiers achieved an accuracy of 97.4%. To enhance automated leukemia diagnosis, Ilyas et al. [18] integrated digital image processing with ML techniques for analyzing blood smear images based on blast cell morphology. Their multi-phase framework involved preprocessing, feature extraction, data preparation, and classification stages. The proposed BC identification model outperformed advanced architectures such as DenseNet121 and EfficientNet, attaining a classification accuracy of 99% for acute leukemia detection.

In another significant contribution, Oktem et al. [19] developed a Surface-Enhanced Raman Spectroscopy (SERS)-based liquid biopsy framework for predicting disease recurrence and classifying AML and ALL subtypes. Different classifiers were evaluated for spectral classification, among which the Random Forest (RF) classifier produced the best performance with an accuracy of 96.1% in recurrence prediction and subtype identification. Feature selection and optimization strategies have also gained considerable attention in leukemia classification tasks. Santhakumar et al. [20] proposed a hybrid Ant Colony Optimization–Ant Lion Optimization (ACO-ALO) technique to enhance classifier efficiency and reduce computational complexity. By integrating SVM for optimal feature selection and classification, the proposed method achieved a prediction accuracy of 93.94%. Focusing on improving sensitivity and specificity, Najjar et al. [21] introduced the Multi-Scale Enhanced EfficientNet framework for detecting subtle variations in ALL images. Their approach incorporated multi-scale feature extraction into the EfficientNetV2B0 architecture, resulting in superior classification performance with an overall accuracy of 98.77%.

Real-time leukemia cell detection has also been explored using advanced object detection frameworks. Ferreira et al. [22] proposed the Y-YOLOv10 model, where Principal Component Analysis (PCA) was

Manuscript received 22 September 2025; Accepted 30 March 2026; Available online 22 November 2026
Digital Object Identifier (**DOI**): https://doi.org/10.35882/jeeemi.v9i1.1224
Copyright © 2026 by the authors. This work is an open-access article and licensed under a Creative Commons Attribution-ShareAlike 4.0 International License (CC BY-SA 4.0).

utilized for dimensionality reduction prior to classification. The YOLOv10-based framework effectively distinguished different types of white blood cells and outperformed models such as YOLOv8 and ResNet50, achieving an average accuracy of 96.85%. In the literature review, current techniques have a number of drawbacks, including biased learning in leukemia categorization, which favors the majority class. This has an impact on the accuracy of diagnosis and treatment decisions by reducing sensitivity to minority leukemia subtypes and raising the rate of misdiagnosis.

This paper presents a novel LEDI-DRCNET approach for classifying images as normal, ALL, AML, or CLL. The blood cell images are denoised using the hybrid filter as average and Laplacian (AVLA) filter to improve the image quality. Adaptive Region-Growing Algorithm (ARGA) is used for segmentation to segment the WBC and RegNet is used to extract the features of WBC. DDRCNN is used to classify as leukemia types and the normal cells and improve the accuracy. Finally, the LEDI-DRCNET model classifies as normal, ALL, AML and CLL. The entire process of the LEDI-DRCNET approach is illustrated in Fig 1.

III. Proposed Methodology

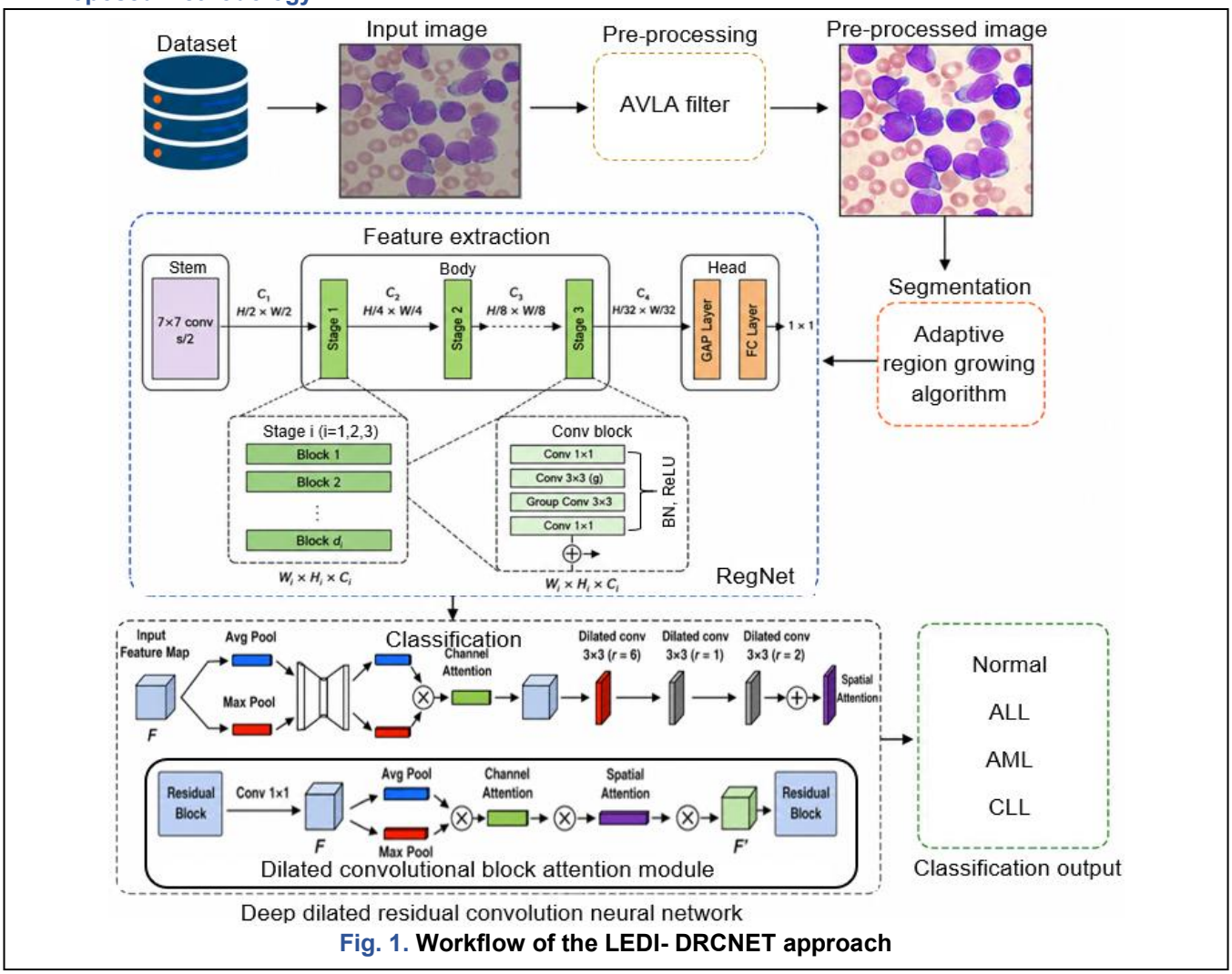


Fig. 1. Workflow of the LEDI- DRCNET approach

A. Dataset description

The ALL-IDB [23] (Acute Lymphoblastic Leukemia Image Database) is a publicly available dataset widely used for the evaluation of automated leukemia detection and classification models. It contains microscopic peripheral blood smear images collected from both healthy individuals and patients diagnosed with Acute Lymphoblastic Leukemia (ALL). The dataset consists of a total of 108 images, including 59 leukemic images and 49 normal images. To facilitate the multi-class classification of Normal, ALL, AML, and CLL categories, additional AML and CLL images were obtained from the AML-Cytomorphology dataset [24] and the American Society of Hematology (ASH) Image Bank [25], respectively. The combined dataset was divided into training and testing sets, with 80% of the

Manuscript received 22 September 2025; Accepted 30 March 2026; Available online 22 November 2026
Digital Object Identifier (**DOI**): https://doi.org/10.35882/jeeemi.v9i1.1224
Copyright © 2026 by the authors. This work is an open-access article and licensed under a Creative Commons Attribution-ShareAlike 4.0 International License (CC BY-SA 4.0).

images allocated for model training and the remaining 20% reserved for testing and validation.

B. Data Augmentation

Image augmentation is an image-processing technique used to artificially increase the size and diversity of training data. Image augmentation is used to overcome the small and uneven datasets used with leukemia classification which may cause overfitting and low generalization.

C. Preprocessing

Average and Laplacian (AVLA) filtering is a hybrid preprocessing technique used to enhance the quality of microscopic blood cell images before further analysis. The average filter is a widely used smoothing method that reduces random noise and intensity variations by replacing each pixel value with the mean of its neighboring pixels, resulting in a smoother image representation. However, smoothing alone may blur important cellular boundaries, which are essential for accurate leukemia detection. The mathematical model is expressed in Eq. (1) [26].

$$Z(m) = \frac{1}{M}\sum_{i=0}^{M-1} y(m-1) \quad (1)$$

where M is the number of pixels in the image, $Z(m)$ is the input, and $y(m-1)$ is the prior input. The edge-detecting Laplacian filters (LF) were used to identify areas that are changing, as BC. The coordinates of the binary matrix are x, y, and the differential second-order equation is represented as $\nabla^2 f$. The differential second-order equation used for edge enhancement is defined in Eq. (2) [26]. Image enhancement is performed using Eq. (3) [27].

$$\nabla^2 f = \frac{\partial^2 f}{\partial^2 x} + \frac{\partial^2 f}{\partial^2 y} \quad (2)$$

$$Enhanced\ image = Z(m) - \nabla^2 f \quad (3)$$

D. Segmentation

The Adaptive Region-Growing Algorithm (ARGA) is an image segmentation technique used to isolate white blood cells from microscopic blood cell images. Region-growing methods operate by selecting initial seed points and progressively expanding the region by including neighboring pixels that exhibit similar intensity and texture characteristics. The homogeneity condition for region segmentation is defined in Eq. (4) [28].

$$|I(x,y) - \mu_R| \leq k.\sigma_R \quad (4)$$

where, $I(x,y)$ is the candidate pixel's intensity, μ_R is the mean intensity of the current region, σ_R is the current region's mean intensity, and k is a tunable threshold constant. Thus, ARGA provides precise boundary detection and reliable separation of leukocyte regions, this is essential for increasing the precision of further feature extraction.

E. Feature extraction

RegNet [29] is a discriminative backbone of segmented white blood cell images on learning discriminative spatial features. RegNet architecture is shown in Fig. 2. The RegNetY-400MF variant was selected for its balance between feature representation capability and computational efficiency. The input images are resized to 224 × 224 × 3 and passed through the convolutional blocks of RegNet, which comprise several stages with progressively increasing channel widths and residual connections.

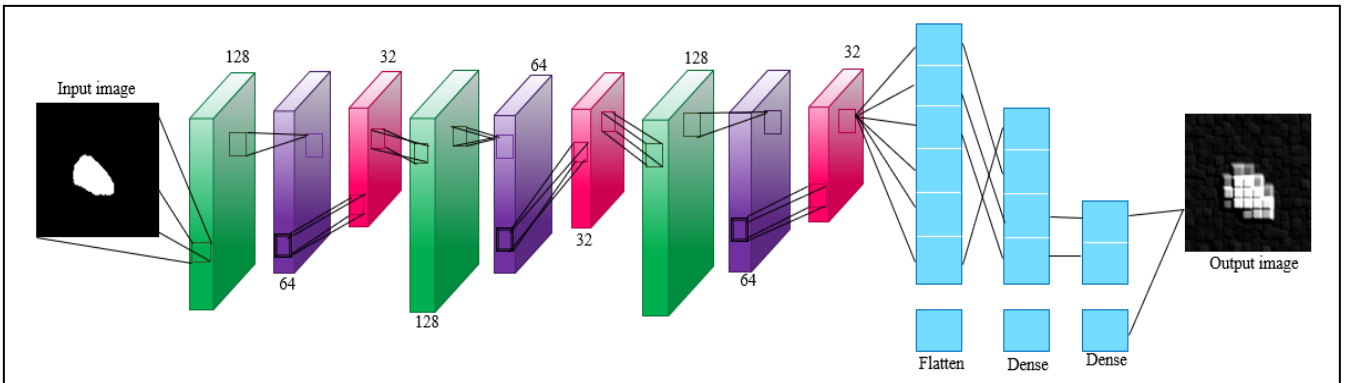


Fig. 2. Architecture of RegNet

The segmented white blood cell images contain significant morphological information such as nucleus shape, chromatin distribution, cytoplasm texture, and cell boundary characteristics. These features are highly important for distinguishing normal cells from leukemia subtypes. During the initial stages of RegNet, low-level image features including edges, intensity variations, contours, and texture patterns are extracted. As the network depth increases, these low-level representations are transformed into high-level semantic features that effectively characterize the structural properties of leukemic cells. The hierarchical feature learning capability of RegNet enables the model to capture both local cellular details and global contextual information simultaneously. Furthermore, the residual connections incorporated within RegNet facilitate efficient information propagation across deep layers and mitigate gradient degradation problems

Manuscript received 22 September 2025; Accepted 30 March 2026; Available online 22 November 2026
Digital Object Identifier (**DOI**): https://doi.org/10.35882/jeeemi.v9i1.1224
Copyright © 2026 by the authors. This work is an open-access article and licensed under a Creative Commons Attribution-ShareAlike 4.0 International License (CC BY-SA 4.0).

during training. Consequently, diagnostically important regions such as nuclei and abnormal cellular structures receive greater attention during the feature extraction process, thereby improving the quality of the learned representations. These compact deep features are subsequently forwarded to the classification stage for leukemia subtype identification. The normalized linear design process of RegNet is formulated in Eq. (5) [30].

$$S_k = \omega_0 + \omega_a . k \ \ for\ 0 \le k \le l \quad (5)$$

where, S_k is width (number of channels) of the kth stage, ω_0 is the initial width, increment per stages is ω_a. The total number of blocks or stages is a l and the stage index is a k. The width scaling strategy employed in RegNet is mathematically represented in Eq. (6) [31].

$$\omega_k = \omega_0 . \omega_m^{rk} \quad (6)$$

A multiplicative step constant is denoted by ω_m, the scaled block index by rk, ω_0 is the initial width and the width at block k by ω_k. T This parameterized scaling strategy enables the network to maintain a balanced trade-off between representational power and computational efficiency. The ability of RegNet to produce regular, hardware-efficient network topologies that are optimized for both speed and accuracy makes it highly suitable for biomedical image analysis applications. Therefore, RegNet serves as an effective feature extraction backbone for capturing discriminative leukemia-related characteristics from segmented blood cell images and improving the overall performance of the proposed leukemia classification framework.

F. Classification

The Deep Dilated Residual Convolutional Neural Network (DDRCNN) [32] is created to be the ultimate classifier which is capable of differentiating the discriminative patterns in the acquired deep features by using the extracted features. The DDRCNN architecture comprises five convolutional blocks: all blocks have 3*3 convolution layer, batch normalization, and ReLU activation to enhance the stability of learning the features. Dilated convolutions with dilation rate of 1, 2 and 4 are used to capture multi-scale contextual information, and the network can expand the receptive field without the need to increase its computational complexity. The convolutional layers have stride = 1 and filter sizes of gradually increasing sizes of 32, 64, 128, 256, 512 feature maps through the stages of the network. DDRCNN architecture is shown in Fig 3. The optimization of the optimal and residual mappings improves learning, as illustrated in Eq. (7) [33].

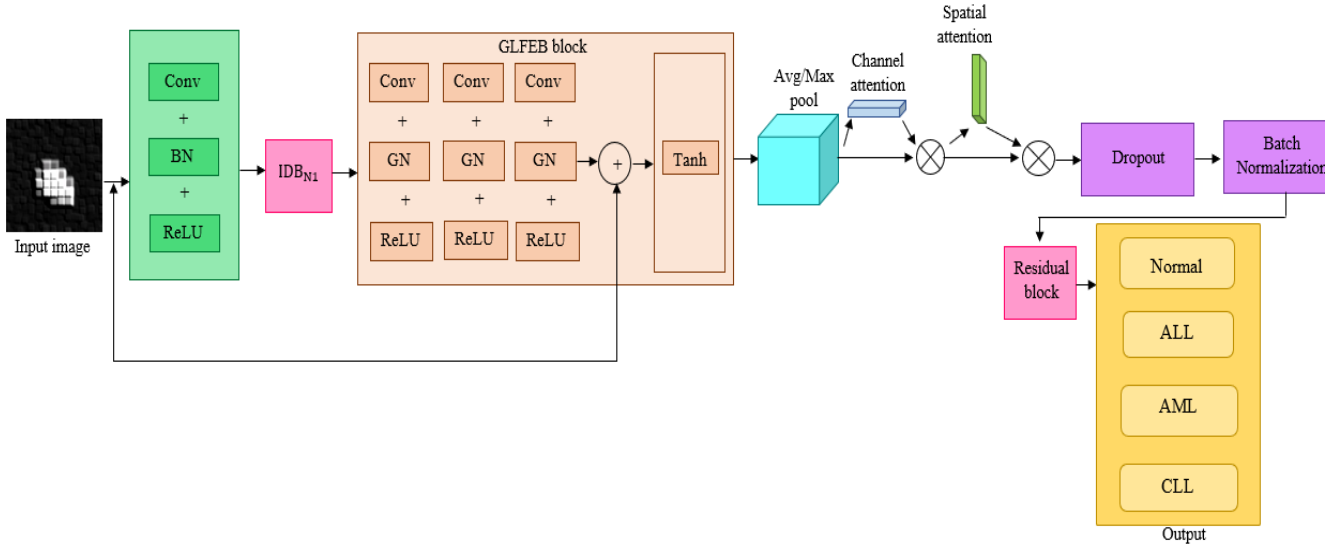


Fig. 3. Architecture of Dilated Deep Residual Convolutional Neural Network

$$O_{RDB} = f_{RDB}(O_{CN}) \quad (7)$$

$$O_{CN} = f_{CN}(I_N) \quad (8)$$

where f_{RDB} denotes Residual Dense Block (RDB) operation, O_{RDB} denotes Output feature map obtained from the Residual Dense Block. This convolution layer (CL) output is denoted by O_{CN}, where I_N denotes the input data and f_{CN} is the function that represents the CL in Eq. (8) [34]. The global features and locally optimized residual features are retrieved using the three-layer GLFEB, where I_N stands for the global and O_{RDB} local features. O_{GLFEB} denotes Output feature map generated by the GLFEB and f_{GLFEB} represents Global and Local Feature Extraction Block operation. The extraction of global and optimized residual features using GLFEB is represented in Eq. (9) [35].

Manuscript received 22 September 2025; Accepted 30 March 2026; Available online 22 November 2026
Digital Object Identifier (**DOI**): https://doi.org/10.35882/jeeemi.v9i1.1224
Copyright © 2026 by the authors. This work is an open-access article and licensed under a Creative Commons Attribution-ShareAlike 4.0 International License (CC BY-SA 4.0).

$$O_{GLFEB} = f_{GLFEB} = (I_N, O_{RDB}) \quad (9)$$

As defined in Eq. (10) [36], the CSAB module generates attentive feature representations from the extracted features. O_{CSAB} denotes Output feature map produced by the CSAB module and f_{CSAB} denotes Channel-Spatial Attention Block operation.

$$O_{CSAB} = f_{CSAB}(O_{CLFEB}) \quad (10)$$

This result is combined with the GLFEB convolution output using element-wise summation to produce elements that improve attentiveness. The final feature group, s_i denotes the set of feature indices belonging to the group, and x_k represents the k-th feature value.

Eq. (12) [37] defines the variance computation for feature normalization

$$Variance(\sigma_i^2) = \frac{1}{m}\sum_{k\epsilon s_i}(x_k - \mu_i)^2 \quad (12)$$

where σ_i^2 denotes the variance of the \(i\)-th normalization group, x_k represents the k-th feature value, μ_i denotes the group mean, and m indicates the number of feature values within the group. Feature normalization is performed according to Eq. (13) [37].

$$feature(\hat{X}_i) = \frac{x_i - \mu_i}{\sqrt{\sigma_i^2 + \epsilon}} \quad (13)$$

where $\hat{X}_i$ denotes the normalized feature value, $x_i$represents the input feature value, μ_i and σ_i^2 indicate the mean and variance of the normalization group, respectively, and ϵ is a small constant introduced to prevent division by zero. The tanh activation function utilized for feature mapping is mathematically expressed in Eq. (14) [37].

$$tanh(F_{GL}) = \frac{e^{F_{GL}} - e^{-F_{GL}}}{e^{F_{GL}} + e^{-F_{GL}}} \quad (14)$$

where F_{GL} represents the global feature representation, e denotes Euler's mathematical constant, and tanh is the hyperbolic tangent activation function that maps the input features to the range [-1,1]. CSAB improves NN ability to extract relevant information from input BCI, allowing them to allocate resources to crucial features in a flexible manner. Global average pooling (GAP) for channel attention is computed using Eq. (15) [38].

$$F_{GAP}(A_t) = \frac{1}{H \times W}\sum_{i=1}^{H}\sum_{j=1}^{W} A_{t,cij} \quad (15)$$

where $F_{GAP}(A_t)$ denotes the global average-pooled feature representation, A_t represents the input feature map, $A_{t,cij}$ denotes the feature value at channel c and spatial position (i,j) and H and W indicate the height and width of the feature map, respectively. The channel attention weight generation process is represented in Eq. (16) [39].

$$(Q_c) = RwLU(W_2 * A_t) \quad (16)$$

where Q_c denotes the channel-attention representation, W_2 represents the learnable weight parameters, * denotes the transformation operation, is normalized using the dropout layer and batch normalization (BN), producing ideal features with good image classification accuracy. Group normalization (GN) occurs when the max pooling layer (MPL) receives the output feature from the CL. The mean calculation used in group normalization is formulated in Eq. (11) [37].

$$Mean(\mu_i) = \frac{1}{m}\sum_{k\epsilon s_i} x_k \quad (11)$$

where μ_i denotes the mean of the i-th normalization group, m represents the number of feature values in the and ReLU is the rectified linear unit activation function. A_t represents the input feature map.

The CA model characteristics are concatenated and provided to fully connected layers before being normalized using the sigmoid function. After processing the $C \times H \times W$, the inter-spatial characteristics (Q_s) produce the $1 \times H \times W$ dimension. The 5×5 convolution kernel's input is normalized using the sigmoid and ReLU activation functions defined by Eq. (17) [40], where W_2 represents the learning parameters.

$$(Q_s) = RwLU(W_2 * A_t) \quad (17)$$

where Q_s denotes the spatial-attention representation, W_2 represents the learnable convolutional weights, * denotes the convolution operation, and A_t represents the input feature map. ReLU denotes the rectified linear unit activation function. The normalization of spatial attention weights is defined in Eq. (18) [41].

$$Q_s^{norm} = \frac{Q_s}{\sum_{c=1}^{C} Q_s} \quad (18)$$

where Q_s^{norm} denotes the normalized spatial-attention representation, Q_s represents the spatial-attention weights, and C indicates the number of feature channels. The denominator represents the sum used to normalize the attention weights across the specified dimension. The CA features and the normalized SA features are combined to get the final attention weights. The input feature map is then subjected to these attention weights in order to highlight spatial locations and informative channels. The DDRCNN classifies images as ALL, AML, CLL, or normal. The proposed LEDI-DRCNET approach is evaluated using recall, specificity, F1-score, accuracy, and precision. Eq. (19), (20), (21), (22) and (23) [42] are utilized to evaluate the overall performance of the proposed leukemia detection framework.

$$accuracy = \frac{TP+TN}{TP+TN+FP+FN} \quad (19)$$

$$Specificity = \frac{TN}{TN+FP} \quad (20)$$

$$Precision = \frac{TP}{TP+FP} \quad (21)$$

$$recall = \frac{TP}{TP+FN} \quad (22)$$

$$f_1 = 2\left(\frac{precision * recall}{precision + recall}\right) \quad (23)$$

Manuscript received 22 September 2025; Accepted 30 March 2026; Available online 22 November 2026
Digital Object Identifier (**DOI**): https://doi.org/10.35882/jeeemi.v9i1.1224
Copyright © 2026 by the authors. This work is an open-access article and licensed under a Creative Commons Attribution-ShareAlike 4.0 International License (CC BY-SA 4.0).

where TP and TN indicates the true positive and negative of the provided images, FP and FN display the sample images false positives and negatives.

IV. Result

This section presents the experimental configuration implemented in MATLAB 2020b and the resulting findings for the LEDI-DRCNET approach.

A. Performance Analysis

The performance of the proposed LEDI-DRCNET framework was evaluated using standard classification metrics, including accuracy, precision, recall, specificity, and F1-score. The experimental results of the proposed framework are illustrated in Fig. 4. The

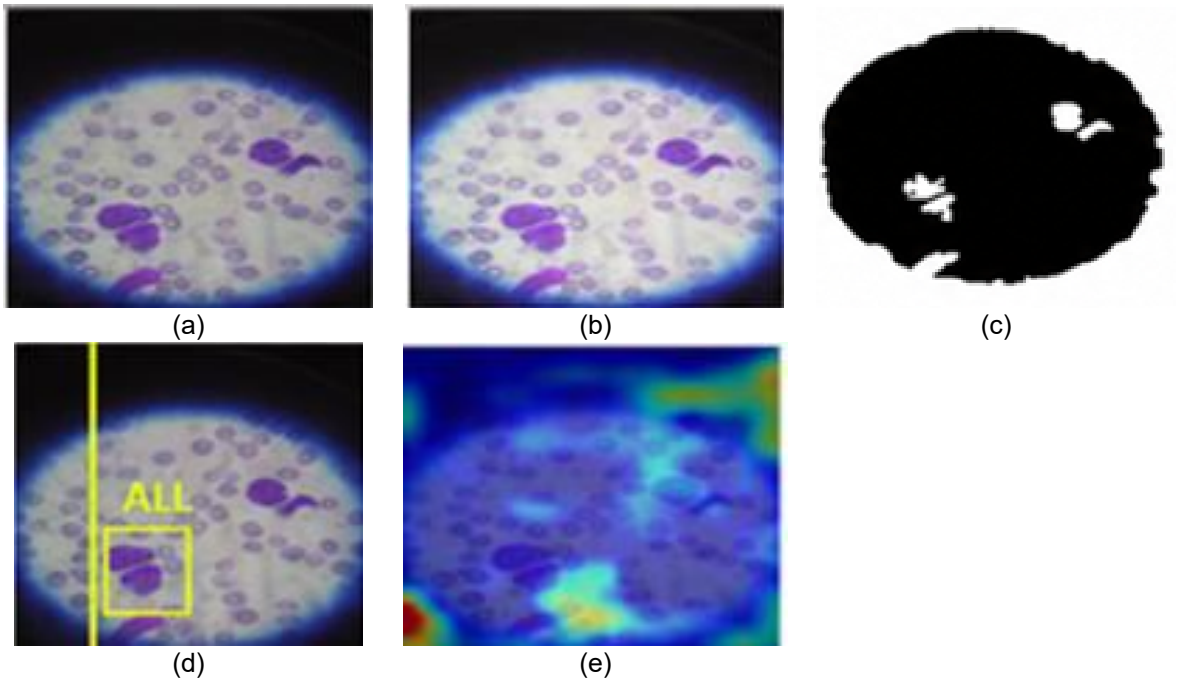


Fig. 4. Experimental result of the LEDI-DRCNET (a) Input image, (b) Preprocessed image, (c) Segmentation result, (d) Classification output, and (e) Grad-CAM visualization

first column shows the original microscopic blood smear images, followed by AVLA preprocessing for noise reduction, ARGA segmentation for WBC isolation, DDRCNN-based leukemia classification, and Grad-CAM visualization highlighting the diagnostically relevant regions influencing the classification decision. The quantitative performance of the proposed framework is summarized in Table 1. The proposed

Fig. 5(a) illustrates the training and validation accuracy curves of the proposed deep learning model, with training epochs on the x-axis and the classification accuracy (%). As the number of training epochs increases, the accuracy gradually improves, indicating that the model effectively learns discriminative features from the blood cell images. Fig. 5(b) presents the training loss curve of the proposed deep learning

Table 1. Performance analysis of the LEDI-DRCNET model

Classes	Accuracy	Specificity	Precision	Recall	F1 score
Normal	99.12%	97.52%	96.23%	98.36%	95.32%
ALL	98.83%	95.25%	94.36%	96.48%	97.26%
AML	99.32%	96.32%	95.21%	93.24%	98.25%
CLL	98.99%	97.98%	96.37%	97.57%	95.53%

LEDI-DRCNET achieved classification accuracies of 99.12%, 98.83%, 99.32%, and 98.99% for the Normal, ALL, AML, and CLL classes, respectively. These results indicate that the proposed framework consistently provides high classification performance across all leukemia categories.

model, with training epochs on the x-axis and the corresponding loss values. The progressive reduction in the loss throughout the training process indicates successful optimization of the network parameters and effective learning of discriminative feature representations. During the initial epochs, the loss

Manuscript received 22 September 2025; Accepted 30 March 2026; Available online 22 November 2026
Digital Object Identifier (**DOI**): https://doi.org/10.35882/jeeemi.v9i1.1224
Copyright © 2026 by the authors. This work is an open-access article and licensed under a Creative Commons Attribution-ShareAlike 4.0 International License (CC BY-SA 4.0).

decreases rapidly as the model captures the underlying characteristics of the input data. The absence of abrupt fluctuations or oscillations further indicates the robustness of the optimization process and the consistency of the training behavior. Ultimately, the further demonstrates that the model effectively minimizes prediction errors while improving its generalization capability.

loss reaches approximately 0.94, indicating effective optimization and satisfactory convergence of the proposed network. The complementary relationship between the continuous reduction in loss and the corresponding improvement in classification accuracy Different Deep Learning Models with the increase in the input size. All models exhibit increasing computational complexity as input size increases, indicating higher computational costs for larger inputs. This fact proves

Table 2. Comparison of the existing model and proposed model

Techniques	Accuracy	Specificity	Precision	Recall	F1 score
EfficientNetV2B3 [16]	97.95%	96.63%	92.05%	94.25%	95.36%
KNN [17]	97.43%	94.56%	96.24%	95.25%	94.11%
DenseNet 121 [18]	99.01%	95.07%	92.37%	96.17%	98.61%
SVM [19]	96.01%	95.26%	90.42%	92.65%	91.36%
Proposed	99.06%	96.76%	95.54%	96.41%	96.59%

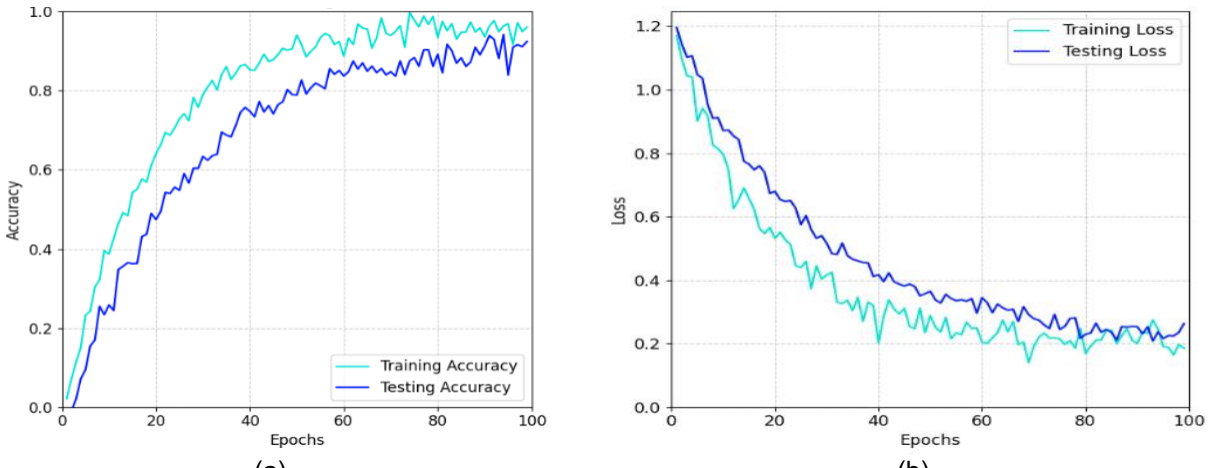
B. Comparative Analysis

The accuracy and efficiency of LEDI-DRCNET were evaluated through comparisons with existing methods. The reported accuracy indicates that the proposed approach outperforms the compared techniques. A comparison is performed between the proposed approach and current approaches such as EfficientNetV2B3 [16], KNN [17], DenseNet 121 [18] and SVM [19]. Table 2 presents the various techniques of the existing model and compare the LEDI-DRCNET model. The LEDI-DRCNET the accuracy 97.95%, 97.43%, 99.01% and 96.01% better than the EfficientNetV2B3 [16], KNN [17], DenseNet 121 [18] and SVM [19] respectively. The LEDI-DRCNET approach achieves an accuracy of 99.06%, outperforming the compared methods. Fig 6 shows the computational of the complexity of Comparison of

the assumption that the proposed model much lessens the computational load without compromising the usefulness of the results in comparison to the standard models like EfficientNetV2B3, KNN, DenseNet121, and SVM.

V. Discussion

The experimental results indicate that the proposed LEDI-DRCNET framework achieved superior leukemia classification performance with an overall accuracy of 99.06%. The high classification accuracy suggests that the integration of AVLA preprocessing, ARGA segmentation, RegNet feature extraction, and DDRCNN classification effectively enhances the



(a) (b)

Fig. 5. Training and testing curve of LEDI-DRCNET (a) Accuracy and (b) loss curve

Manuscript received 22 September 2025; Accepted 30 March 2026; Available online 22 November 2026
Digital Object Identifier (**DOI**): https://doi.org/10.35882/jeeemi.v9i1.1224
Copyright © 2026 by the authors. This work is an open-access article and licensed under a Creative Commons Attribution-ShareAlike 4.0 International License (CC BY-SA 4.0).

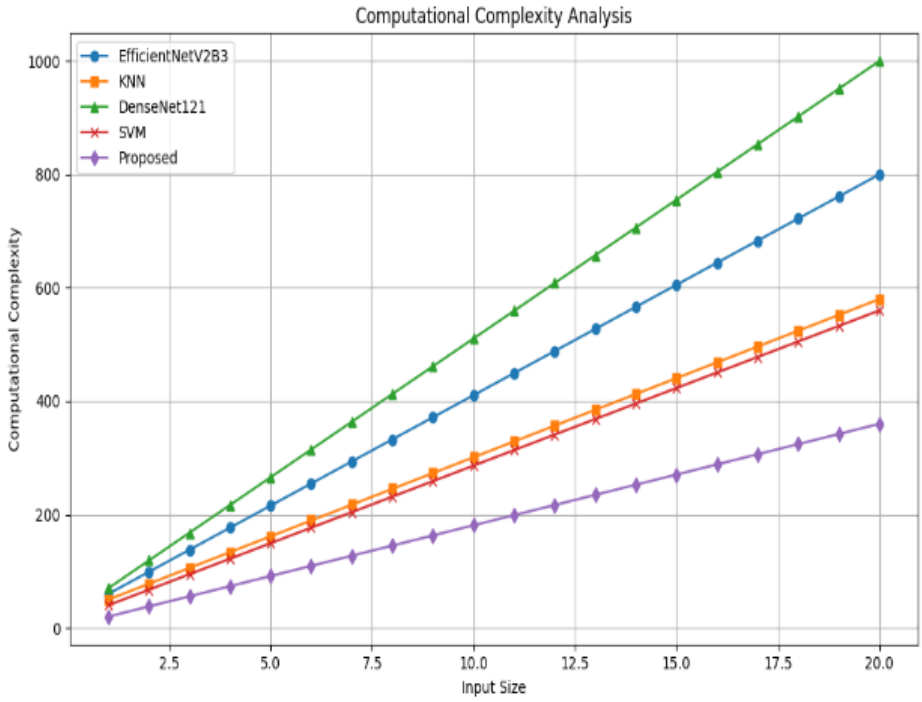


Fig. 6. Computational Complexity Comparison of Different Deep Learning Models.

Table 3. Accuracy comparison of proposed LEDI-DRCNET method with existing method

Authors	Method	Accuracy	p-value
Santhakumar et al., [20]	ACO-ALO	93.94%	0.036
Najjar et al., [21]	EfficientNet	98.77%	0.058
Ferreira et al., [22]	Y-YOLOv10	96.85%	0.072
Proposed	LEDI-DRCNET	99.06%	0.008

discriminative representation of leukemia cell images. The AVLA filtering stage significantly contributed to noise reduction and edge enhancement, which improved the visibility of white blood cell boundaries and enabled accurate segmentation. Similarly, the adaptive behavior of the ARGA segmentation algorithm effectively handled overlapping and irregularly shaped leukocyte regions, leading to more precise extraction of region-based features. The RegNet feature extraction model played a major role in improving classification performance by capturing multi-scale spatial and structural information from blood cell images. Unlike conventional handcrafted feature extraction methods, RegNet automatically learned discriminative deep representations that improved the differentiation between normal cells and leukemia subtypes such as ALL, AML, and CLL.

The training and validation accuracy curves indicate that the proposed model achieved stable convergence with minimal fluctuations, indicating good generalization capability and reduced overfitting. In addition, the gradual reduction in loss values confirms the effectiveness of the optimization strategy and stable learning behavior of the DDRCNN. The ROC analysis validates the robustness of the proposed framework, where all leukemia classes achieved high AUC values close to 1.0, demonstrating strong sensitivity and specificity for leukemia classification.

Although all the compared methods in Table 2 were developed for automated leukemia classification using microscopic blood smear images, they differ in their feature extraction and classification strategies. EfficientNetV2B3 [16] and DenseNet121 [18] employ deep convolutional networks for feature learning, similar to the proposed framework. However, the proposed LEDI-DRCNET integrates AVLA preprocessing and ARGA segmentation before RegNet-based feature extraction, enabling improved preservation of cellular boundaries and more discriminative feature representations. The KNN [17]

Manuscript received 22 September 2025; Accepted 30 March 2026; Available online 22 November 2026
Digital Object Identifier (**DOI**): https://doi.org/10.35882/jeeemi.v9i1.1224
Copyright © 2026 by the authors. This work is an open-access article and licensed under a Creative Commons Attribution-ShareAlike 4.0 International License (CC BY-SA 4.0).

and SVM [19] methods rely on conventional machine learning classifiers, which have limited capability to model complex morphological variations in leukemia cells. In contrast, the proposed DDRCNN incorporates dilated convolutions and residual learning to capture multi-scale contextual information while maintaining efficient gradient propagation. These architectural differences enable the proposed framework to achieve higher accuracy of 99.06% than EfficientNetV2B3 of 97.95%, KNN of 97.43%, DenseNet121 of 99.01% and SVM of 96.01% demonstrating its superior capability for robust leukemia subtype classification.

Furthermore, the integration of preprocessing, segmentation, and advanced feature learning contributes to the effective identification of important cellular characteristics. The proposed framework enhances the discrimination of subtle morphological differences among leukemia subtypes, thereby improving classification reliability. Overall, the comparative results highlight the effectiveness of the proposed approach in achieving accurate and consistent automated leukemia detection. Table 3 demonstrates the comparison of the accuracy of existing methods and the LEDI-DRCNET method. Compared with the ACO-ALO approach proposed by Santhakumar et al. [20], the proposed method improved classification accuracy by 5.45%. Similarly, the proposed model achieved better performance than the EfficientNet framework introduced by Najjar et al. [21] and the Y-YOLOv10 approach proposed by Ferreira et al. [22]. Despite achieving promising classification performance, the proposed framework has certain limitations. The proposed model was evaluated using a relatively small and less diverse dataset, which may affect the generalization capability of the framework in real-world clinical environments. In addition, the classification performance is highly dependent on image quality, illumination conditions, and staining variations in microscopic blood smear images. The proposed approach may also experience difficulties when processing highly complex overlapping leukocyte structures or noisy samples. Furthermore, the computational requirements of deep learning models remain higher than traditional machine learning approaches, which may limit deployment in low-resource healthcare systems.

VI. Conclusion

In this research, a novel LEDI-DRCNET was proposed for the LD classification using a DDRCNN. Initially, the input images are denoised using the AVLA filter to improve the image quality and edge detection. ARGA is used to segment WBCs in the images. RegNet was used to extract WBC features, and DDRCNN was used for the classification of leukemia to improve performance. Finally, DDRCNN classifies the images as normal, ALL, AML, or CLL. The LEDI-DRCNET approach accomplishes a higher AC of 99.06%. The LEDI-DRCNET improves the AC range by 1.13%, 1.67%, 0.05%, and 3.17% better than EfficientNetV2B3, KNN, DenseNet 121, and SVM, respectively. The proposed model is limited by a relatively small and less diverse dataset, which may affect generalization and lead to overfitting in real-world scenarios. It also depends heavily on image quality and may struggle with complex. Future research may focus on larger and more diverse datasets, improving reliability for clinical applications, and increasing robustness to real-world variability.

Acknowledgment

The author expresses gratitude to the supervisor for guidance and support throughout this research.

Funding

Not applicable.

Data Availability

The datasets used in this study were obtained from publicly available repositories and can be accessed through the following sources:

- ALL-IDB Dataset (Normal and ALL): https://scotti.di.unimi.it/all/
- AML-Cytomorphology Dataset (AML): https://www.cancerimagingarchive.net/collection/aml-cytomorphology_lmu/
- American Society of Hematology Image Bank (CLL): https://imagebank.hematology.org/

The combined dataset consists of Normal, ALL, AML, and CLL microscopic blood smear images used for the training and evaluation of the proposed LEDI-DRCNET model.

Author Contribution

Della Reasa Valiaveetil contributed to conceptualization, methodology, data preparation, model development, analysis, and manuscript drafting. Kanimozhi T supervised the study, reviewed the methodology, validated the results, and revised the manuscript. All authors reviewed and approved the final manuscript.

Declarations

Ethical Approval

Ethical approval was not required because this study used a publicly available anonymized dataset and did not involve direct human participants or identifiable personal data.

Consent for Publication

Consent for publication was not required because the study used publicly available anonymized image data.

Competing Interests

Manuscript received 22 September 2025; Accepted 30 March 2026; Available online 22 November 2026
Digital Object Identifier (**DOI**): https://doi.org/10.35882/jeeemi.v9i1.1224
Copyright © 2026 by the authors. This work is an open-access article and licensed under a Creative Commons Attribution-ShareAlike 4.0 International License (CC BY-SA 4.0).

The authors declare that they have no competing interests.

Declaration of Generative AI in Scholarly Writing: The authors declare that no generative AI or AI-assisted technologies were used in the preparation of this manuscript.

References

[1] M. Ilyas, M. Ramzan, M. Deriche, K. Mahmood, and A. Naz, "An efficient leukemia prediction method using machine learning and deep learning with selected features," *PLoS One*, vol. 20, no. 5, pp. e0320669, 2025, doi: 10.1371/journal.pone.0320669

[2] N.O. Adiwijaya, S. Ardiansyah, and D.I. Swasono, "Detecting acute lymphoblastic leukemia in blood smear images using CNN and SVM," *Kinetik: Game Technology, Information System, Computer Network, Computing, Electronics, and Control*, 2025, doi: 10.22219/kinetik.v10i1.2027

[3] K. Pritee, and R.D. Garg, "Optimized convolutional neural network model for multilevel classification in leukemia diagnosis using Tversky loss," *Artificial Intelligence in Health*, pp. 4710, 2025, doi: 10.36922/aih.4710

[4] M. Zolfaghari, and H. Sajedi, "A survey on automated detection and classification of acute leukemia and WBCs in microscopic blood cells," *Multimedia Tools and Applications*, vol. *81*, no. 5, pp. 6723-6753, 2022. doi:10.1007/s11042-022-12108-7

[5] G. Yan, G. Mingyang, S. Wei, L. Hongping, Q. Liyuan, L. Ailan, K. Xiaomei, Z. Huilan, Z. Juanjuan, and Q. Yan, "Diagnosis and typing of leukemia using a single peripheral blood cell through deep learning," *Cancer Science*, 2025, doi: 10.1111/cas.16374

[6] G. Sriram, T.G. Babu, R. Praveena, and J.V. Anand, "Classification of leukemia and leukemoid using VGG-16 convolutional neural network architecture," *Molecular & Cellular Biomechanics*, vol. *19*, no. 1, pp. 29, 2022. doi:10.32604/mcb.2022.016966

[7] A. Ahilan, J. Angel Sajani, A. Jasmine Gnana Malar, and B. Muthu Kumar, "Machine Learning-Based Brain Disease Classification Using EEG and MEG Signals," In *International Conference on Frontiers of Intelligent Computing: Theory and Applications*, pp. 487-498, 2023, doi: 10.1007/978-981-99-6702-5_40

[8] J. Angel Sajani, and A. Ahilan, "Classification of brain disease using deep learning with multi-modality images," *Journal of Intelligent & Fuzzy Systems*, vol. 45, no. 2, pp. 3201-3211, 2023, doi: 10.3233/jifs-230090

[9] P.K. Das, B. Sahoo, and S. Meher, "An efficient detection and classification of acute leukemia using transfer learning and orthogonal softmax layer-based model," *IEEE/ACM Transactions on Computational Biology and Bioinformatics*, vol. *20*, no. 3, pp.1817-1828, 2022. doi: 10.1109/TCBB.2022.3218590

[10] A. Bindhu, A. Ahilan, S. Vallisree, P. Maria Jesi, B. Muthu Kumar, N.K. Marriwala, and A.Q.M. Sabr, "Skin Cancer Diagnosis Using High-Performance Deep Learning Architectures," In *International Conference on Emergent Converging Technologies and Biomedical Systems*, pp. 693-703, 2023, doi: 10.1007/978-981-99-8646-0_54

[11] A. Geetha, M.C. Sobia, D. Santhi, and A. Ahilan, "DEEP GD: Deep learning-based snapshot ensemble CNN with EfficientNet for glaucoma detection," *Biomedical Signal Processing and Control*, vol. 100, pp. 106989, 2025, doi: 10.1016/j.bspc.2024.106989

[12] R. Baig, A. Rehman, A. Almuhaimeed, A. Alzahrani, and H.T. Rauf, "Detecting malignant leukemia cells using microscopic blood smear images: a deep learning approach," *Applied Sciences*, vol. *12*, no. 13, pp.6317, 2022. doi:10.3390/app12136317

[13] M. Roshal, and Q. Gao, "Flow cytometry evaluation of acute myeloid leukemia minimal residual disease based on an understanding of the normal maturation patterns in the blast compartments," *American Journal of Clinical Pathology*, vol. 163, no. 5, pp. 775-793, 2025, doi: 10.1093/ajcp/aqae187

[14] A.E. Aby, S. Salaji, K.K. Anilkumar, and T. Rajan, "Classification of acute myeloid leukemia by pre-trained deep neural networks: A comparison with different activation functions," *Medical Engineering & Physics*, vol. 135, pp. 104277, 2025, doi: 10.1016/j.medengphy.2024.104277

[15] S. Saleem, J. Amin, M. Sharif, G.A. Mallah, S. Kadry, and A.H. Gandomi, "Leukemia segmentation and classification: A comprehensive survey," *Computers in biology and medicine*, vol. *150*, pp.106028, 2022.

[16] S.T.S. Darmawan, and N.H. Shabrina, "Explainable deep learning for diagnosing acute lymphocytic leukemia using blood smear images," *Bulletin of Electrical Engineering and Informatics*, vol. 14, no. 2, pp. 1298-1307, 2025, doi: 10.11591/eei.v14i2.9073

Manuscript received 22 September 2025; Accepted 30 March 2026; Available online 22 November 2026
Digital Object Identifier (**DOI**): https://doi.org/10.35882/jeeemi.v9i1.1224
Copyright © 2026 by the authors. This work is an open-access article and licensed under a Creative Commons Attribution-ShareAlike 4.0 International License (CC BY-SA 4.0).

[17] H. Almahdawi, A. Akbas, and J. Rahebi, "Deep learning neural network based on PSO for leukemia cell disease diagnosis from microscope images," *Journal of Imaging Informatics in Medicine*, pp. 1-10, 2025, doi: 10.1007/s10278-025-01474-x

[18] M. Ilyas, M. Bilal, N. Malik, H.U. Khan, M. Ramzan, and A. Naz, "Using Deep Learning Techniques to Enhance Blood Cell Detection in Patients with Leukemia," *Information*, vol. 15, no. 12, pp. 787, 2024, doi: 10.3390/info15120787

[19] F. Oktem, M. Akdeniz, Z. Al-Shaebi, G. Akyol, M. Keklik, and O. Aydin, "SERS and Machine Learning-Enabled Liquid Biopsy: A Promising Tool for Early Detection and Recurrence Prediction in Acute Leukemia," *ACS omega*, vol. 10, no. 12, pp. 11887-11899, 2025, doi: 10.1021/acsomega.4c08499

[20] D. Santhakumar, G. Rajaram, R. Elankavi, J. Viswanath, I. Govindharaj, and J. Raja, "Enhanced leukemia prediction using hybrid ant colony and ant lion optimization for gene selection and classification," *MethodsX*, vol. 14, pp. 103239, 2025, doi: 10.1016/j.mex.2025.103239

[21] F.H. Najjar, S. Abd Kadum, and N.B. Hassan, "Integrating Multi-scale Feature Extraction into EfficientNet for Acute Lymphoblastic Leukemia Classification," *Journal of Image and Graphics*, vol. 13, no. 1, 2025, doi: 10.18178/joig.13.1.83-89

[22] F.R.T. Ferreira, and L.M. do Couto, "Using deep learning on microscopic images for white blood cell detection and segmentation to assist in leukemia diagnosis," *The Journal of Supercomputing*, vol. 81, no. 2, pp. 1-42, 2025, doi: 10.1007/s11227-024-06903-2

[23] R. Arif, S. Akbar, A.B. Farooq, S.A. Hassan, and S. Gull, "Automatic detection of leukemia through convolutional neural network," In 2022 International Conference on Frontiers of Information Technology (FIT), pp. 195-200, 2022. IEEE.

[24] Z.A. Ibrahim, and M.A.J. Al-Sambawee, "Clinical readiness and limitations of artificial intelligence in hematologic diagnostics: a critical analytical review," Discover Artificial Intelligence, vol. 6. no. 1, pp. 223, 2026. doi:10.1007/s44163-026-00956-3

[25] A. Rehman, T. Meraj, A.M. Minhas, A. Imran, M. Ali, and W. Sultani, "A large-scale multi domain leukemia dataset for the white blood cells detection with morphological attributes for explainability," In International Conference on Medical Image Computing and Computer-Assisted Intervention, pp. 553-563, 2024. Cham: Springer Nature Switzerland. doi:10.3390/app12136317

[26] S.S. Khan, M. Khan, and Y. Alharbi, "Fast local laplacian filter based on modified laplacian through bilateral filter for coronary angiography medical imaging enhancement," *Algorithms*, vol. *16*, no. 12, p.531, 2023. doi:10.3390/a16120531

[27] K.M. Veena, G.V. Aryan, V. Mayya, R.N. Raj, and S.V. Bhandary, "A Comprehensive Study of Preprocessing Influence on Diabetic Retinopathy Detection," In *2025 IEEE International Conference on Distributed Computing, VLSI, Electrical Circuits and Robotics (DISCOVER)*, pp. 1-6, IEEE. 2025. doi:10.1109/DISCOVER66922.2025.11259013

[28] E.B. Kayal, S. Ganguly, A. Sasi, D.S. Dheeksha, M. Saini, S. Sharma, S. Gupta, N. Sharma, K. Rangarajan, S. Bakhshi, and D. Kandasamy, "3D Segmentation of Whole Lung and Metastatic Lung Nodules Using Adaptive Region Growing and Shape-based Morphology," *Journal of Computer Assisted Tomography*, vol. *49*, no. 4, pp.611-624, 2025. doi:10.1097/RCT.0000000000001719

[29] A.H. Efat, "Chi 2 weighted ensemble: A multi-layer ensemble approach for skin lesion classification using a novel framework-optimized regnet synergy with attention-triplet," PloS one, vol. 20, no. 5, pp. e0321803, 2025. doi: 10.1371/journal.pone.0321803

[30] J. Mahawar, A. Verma, B. Sandik, and M. Mishra, "RegNet-based Approach for the Detection of Skin Diseases," In *2026 International Conference on Computing, Electronics & Communications Engineering (ICCECE)*, pp. 1-6, 2026. doi:10.1109/ICCECE69715.2026.11492946.

[31] A.B.M. Arif, A.D. Kotian, A.B. BR, G. Sherigar, and S.J. Bhat, "Comparative Evaluation of RegNet Architectures for Multi-Task Skin Cancer Detection," In *2025 IEEE Pune Section International Conference (PuneCon)*, pp. 1-5. 2025. IEEE. doi:10.1109/PuneCon67554.2025.11377944

[32] F. Ahmad, W. Hou, J. Xiong, and Z. Xia, "Fully automated cardiac MRI segmentation using dilated residual network," *Medical Physics*, vol. *50*, no. 4, pp. 2162-2175, 2023. doi:10.1002/mp.16108

[33] S. Athisayamani, R.S. Antonyswamy, V. Sarveshwaran, M. Almeshari, Y. Alzamil, and V. Ravi, "Feature extraction using a residual deep convolutional neural network (ResNet-152) and optimized feature dimension reduction for MRI

Manuscript received 22 September 2025; Accepted 30 March 2026; Available online 22 November 2026
Digital Object Identifier (**DOI**): https://doi.org/10.35882/jeeemi.v9i1.1224
Copyright © 2026 by the authors. This work is an open-access article and licensed under a Creative Commons Attribution-ShareAlike 4.0 International License (CC BY-SA 4.0).

brain tumor classification," *Diagnostics*, vol. *13*, no. 4, pp.668, 2023. doi:10.3390/diagnostics13040668

[34] R. Kashyap, "Stochastic dilated residual ghost model for breast cancer detection," *Journal of Digital Imaging*, vol. *36*, no. 2, pp. 562-573. 2023. doi:10.1007/s10278-022-00739-z

[35] M. Zhou, Y. Zhang, X. Xu, J. Wang, and F. Khalvati, "Edge-enhanced dilated residual attention network for multimodal medical image fusion," In *2024 IEEE International Conference on Bioinformatics and Biomedicine (BIBM)*, pp. 4108-4111, 2024. IEEE. doi:10.1109/BIBM62325.2024.10821967

[36] A.E. Ahmed, Q. Abbas, Y. Daadaa, I. Qureshi, G. Perumal, and M.E. Ibrahim, "A residual-dense-based convolutional neural network architecture for recognition of cardiac health based on ECG signals," *Sensors*, vol. *23*, no. 16, pp.7204, 2023. doi:10.3390/s23167204

[37] A. Naveed, S.S. Naqvi, T.M. Khan, S. Iqbal, M.Y. Wani, and H.A. Khan, "AD-Net: Attention-based dilated convolutional residual network with guided decoder for robust skin lesion segmentation," *Neural Computing and Applications*, vol. *36*, no. 35, pp.22277-22299, 2024. doi:10.1007/s00521-024-10362-4

[38] H. Polat, "Multi-task semantic segmentation of CT images for COVID-19 infections using DeepLabV3+ based on dilated residual network," *Physical and Engineering Sciences in Medicine*, vol. *45*, no. 2, pp. 443-455, 2022. doi:10.1007/s13246-022-01110-w

[39] J. Fang, X. Ning, T. Mao, M. Zhang, Y. Zhao, S. Hu, and J. Wang, "A multi-focus image fusion network combining dilated convolution with learnable spacings and residual dense network," *Computers and Electrical Engineering*, vol. *117*, pp.109299, 2024. doi: 10.1016/j.compeleceng.2024.109299

[40] A. Sahu, K.P.S. Rana, and V. Kumar, "An application of deep dual convolutional neural network for enhanced medical image denoising," *Medical & Biological Engineering & Computing*, vol. *61*, no. 5, pp. 991-1004, 2023. doi:10.1007/s11517-022-02731-9

[41] X. Li, H. Zhang, H. Yang, and T.Q. Li, "CS-MRI reconstruction using an improved GAN with dilated residual networks and channel attention mechanism," *Sensors*, vol. *23*, no. 18, pp. 7685, 2023. doi:10.3390/s23187685

[42] K.M. Sujon, R. Hassan, K. Choi, and M.A. Samad, "Accuracy, precision, recall, f1-score, or MCC? empirical evidence from advanced statistics, ML, and XAI for evaluating business predictive models," Journal of Big Data, vol. 12, no. 1, pp.268, 2025. doi:10.1186/s40537-025-01313-4

Author Biography



Della Reasa Valiaveetil has completed B.Tech. degree in electronics and communication engineering from Sahrdaya College of Engineering, Kodakara affiliated to University of Calicut, India in 2010 and completed M.E in communication systems at Hindusthan College of Engineering, Coimbatore, affiliated to Anna University, Tamilnadu, India in 2012. She is currently working as assistant professor in the Department of Electronics and Communication Engineering at Christ College of Engineering, Irinjalakuda, Kerala, India and pursuing Ph.D. at Vel Tech Rangarajan Dr. Sagunthala R&D Institute of Science and Technology, Avadi, Chennai, Tamil Nadu. Areas of interest are digital image processing, digital communication, wireless communication. She can be contacted at email: dellareasa@gmail.com.



Kanimozhi T received the Ph.D. degree in information and communication engineering from Anna University, Chennai, India, in 2016. She is currently a professor with the Department of Electronics and Communication Engineering, Vel Tech Rangarajan Dr. Sagunthala Research and Development Institute of Science and Technology, Avadi, Chennai. Her research interests include deep learning, soft computing, image processing, quantum computing, and sensors. She can be contacted at email: drtkanimozhi@veltech.edu.in.

Manuscript received 22 September 2025; Accepted 30 March 2026; Available online 22 November 2026
Digital Object Identifier (**DOI**): https://doi.org/10.35882/jeeemi.v9i1.1224
Copyright © 2026 by the authors. This work is an open-access article and licensed under a Creative Commons Attribution-ShareAlike 4.0 International License (CC BY-SA 4.0).